



You have downloaded a document from
RE-BUŚ
repository of the University of Silesia in Katowice

Title: Styrene epoxidation over heterogeneous manganese(III) complexes

Author: Iwona Kuźniarska-Biernacka, Agata Lisińska-Czekaj, Dionizy Czekaj, Maria José Alves, Antonio Mauricio Fonseca, Isabel Correia Neves

Citation style: Kuźniarska-Biernacka Iwona, Lisińska-Czekaj Agata, Czekaj Dionizy, José Alves Maria, Mauricio Fonseca Antonio, Correia Neves Isabel. (2016). Styrene epoxidation over heterogeneous manganese(III) complexes. "Archives of Metallurgy and Materials" (2016, iss. 3, s. 1477-1482), doi 10.1515/amm-2016-0242



Uznanie autorstwa - Użycie niekomercyjne - Bez utworów zależnych Polska - Licencja ta zezwala na rozpowszechnianie, przedstawianie i wykonywanie utworu jedynie w celach niekomercyjnych oraz pod warunkiem zachowania go w oryginalnej postaci (nie tworzenia utworów zależnych).



UNIwersYTET ŚLĄSKI
W KATOWICACH



Biblioteka
Uniwersytetu Śląskiego



Ministerstwo Nauki
i Szkolnictwa Wyższego

I. KUŹNIARSKA-BIERNACKA*^{#1}, A. LISINSKA-CZEKAJ**[#], D. CZEKAJ**[#], M. JOSÉ ALVES*, A. MAURICIO FONSECA*, I. CORREIA NEVES*[#]

STYRENE EPOXIDATION OVER HETEROGENEOUS MANGANESE(III) COMPLEXES

The manganese(III) complex functionalised with 2,3-dihydropyridazine has been encapsulated in the supercages of the NaY zeolite using two different procedures, flexible ligand and *in situ* complex. The parent zeolite and the encapsulated manganese(III) complexes were screened as catalysts for styrene oxidation by using *t*-BOOH as the oxygen source in acetonitrile. Under the optimized conditions, the catalysts exhibited moderate activity with high selectivity to benzaldehyde

1. Introduction

A large number of transition metal complexes have been supported on a variety of materials ranging from polymers to mesoporous silica to act as catalysts. Various immobilization strategies for Mn(III)–salen complexes involving multi-step surface modification of the support and its binding to the catalytically active complex are reported in the literature [1, 2]. Although complex immobilization has sometimes been shown to increase the activity of homogeneous catalysts [3, 4], it usually also induces an increase in the reaction time as a consequence of the diffusion constraints promoted by the porous structure of the supports.

In this connection it is worth to mention that the microporous structures called zeolites can be produced, containing cages and channels within the structure (Fig. 1). They have many important industrial applications due to their unique architecture; they can be used as sieves to purify water, to separate out molecules of different sizes, to make detergents for the kitchen, to remove radio-active elements from spent nuclear fuel, and as catalysts for many chemical reactions, especially in the petro-chemical industry.

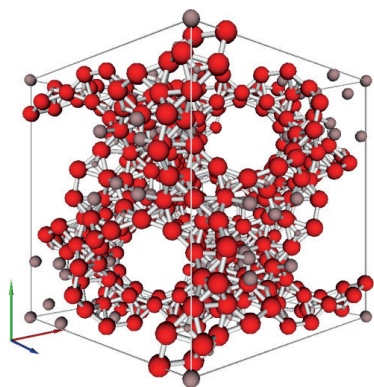


Fig. 1. NaY zeolite structure with cages and channels

It was found that Mn(III) complexes with N_2O_2 Schiff base (usually denoted as salen ligands) show catalytic activity in C=C oxidation under homogeneous [5,6] as well as heterogeneous conditions [7,9] being Mn(V) (oxo) species the active oxidant [10,11]. Several oxygen sources have been used for the oxidation of alkenes via Mn(III)–salen complexes, such as iodosylbenzene, 3-chloroperoxybenzoic acid, sodium hypochlorite, dioxygen, dry air, hydrogen peroxide and *tert*-butylhydroperoxide. [10, 12, 13]. Many scientists have studied the catalytic reaction conditions, formation of intermediates as well as products [e.g. 14,15], they are strongly dependent on the oxygen donor, solvent and the metal complex, particularly the ligand, due to this different steric and electronic properties [11, 16]. No literature data was yet found on dihydropyridazine complexes.

In this work, we describe the preparation of the heterogeneous catalysts based in a manganese complex entrapped in the zeolite structure and the study of the catalytic properties of styrene oxidation, with different solvents.

2. Experimental

2.1. Materials and methods

Prior to use, NaY zeolite (CBV100, Si/Al ratio = 2.83, Zeolyst International) in powder form was calcined at 500 °C during 8 h under a dry air stream. All chemicals and solvents used were reagent grade and purchased from Aldrich: 2-hydroxyphenylaldehyde; manganese(II) chloride tetrahydrate ($MnCl_2 \times 4H_2O$); manganese(II) sulphate monohydrate ($MnSO_4 \times H_2O$); triethylamine; acetonitrile; dichloromethane; ethanol; *tert*-butyl hydroperoxide solution – 5.0–6.0 M in decane (*t*BuOOH); sodium hypochlorite (NaOCl); hydrogen peroxide solution – 30 wt% in water; chlorobenzene (PhCl); and styrene. Potassium bromide

* DEPARTAMENTO DE QUÍMICA, CENTRO DE QUÍMICA, UNIVERSIDADE DO MINHO, 4710-057 BRAGA, PORTUGAL

¹ CURRENT ADDRESS: DEPARTAMENTO DE QUÍMICA E BIOQUÍMICA FACULDADE DE CIÊNCIAS DA UNIVERSIDADE DO PORTO, RUA DE CAMPO ALEGRE, 4169-007 PORTO, PORTUGAL

** UNIVERSITY OF SILESIA, INSTITUTE OF TECHNOLOGY AND MECHATRONICS, 41-200 SOSNOWIEC, 12 ŻYTNIA STR., POLAND

[#] Corresponding author: iwonakb@fc.u.pt, ineves@quimica.uminho.pt

(spectroscopic grade) used for FTIR analysis was purchased from Merck.

2.2. Methods

Quantitative analysis of Mn was carried out by inductively coupled plasma atomic emission spectrometry (ICP-AES) using a Philips ICP PU 7000 spectrometer. Elemental analysis (C, H, N) were determined using a Leco CHNS-932 analyser. Room-temperature FTIR spectra of solids were obtained from powdered samples mixed with KBr, using a Bomem MB104 spectrophotometer. The electronic spectra were obtained using Shimadzu UV/3101 PC spectrophotometer. X-ray diffraction (XRD) patterns were recorded using a Philips analytical X-ray model PW1710 BASED diffractometer system. All the samples were powdered and quartz powder was added as an internal standard. Measurements were performed at room temperature under the following conditions: CuK α radiation was used (λ_{α_1} =1.54056 Å; λ_{α_2} =1.54439 Å; ratio α_{21} =0.5); divergence slit automatic L =10mm (L =12mm for NaY sample); receiving slit 0.10 (0.2 for NaY sample); monochromator was used; data angle range 2θ =2.01 – 64.99°; detector scan step size $\Delta 2\theta$ =0.02°; scan type continuous; scan step time t =1.25s). Analysis of the X-ray diffraction patterns was carried out using X'pert HighScore Plus software (PANalytical B.V). The latest available ICSD [17] database was utilized. Scanning electron microscope (SEM) images were obtained using a Leica Cambridge S360 scanning microscope equipped with an EDS system. Before examination, the samples were coated with gold under vacuum to avoid surface charging using a Fisons Instruments SC502 sputter coater. Gas chromatography–flame ionization (GC-FID) chromatograms were obtained in an SRI 8610C chromatograph equipped with a CP-Sil 8CB capillary column. Nitrogen was used as the carrier gas.

2.3. Catalytic oxidation of styrene

The epoxidation of styrene was studied at room temperature under constant stirring. Briefly, 0.1 g (1.0 mmol) styrene, 0.1 g (1.0 mmol) chlorobenzene (internal standard) and 0.10 g heterogeneous catalyst were mixed in 5.0 mL acetonitrile; *t*-BuOOH (0.3 mL, 1.65 mmol, of 5.5 M decane solution) was progressively added to the reaction medium 0.05 mL min⁻¹. The blank experiment was run under the same conditions excluding the catalyst. The identification of reaction products was confirmed by comparison with authentic samples, by GC. After the reaction cycle, the catalysts were washed, dried and characterized.

2.4. Synthesis of (S)-6-(hydroxymethyl)-N-phenyl-2,3-dihydropyridazine-1(6H)-carboxamide

Synthesis of the ligand was done as described in previously work [18]. Briefly, to the levorotatory esterisomer [18] solubilized in dry THF was added LiAlH₄ in THF, at

0 °C. The mixture was stirring. The portion of water was added, and the mixture was extracted with ethyl acetate. The organic layers were washed with saturated aqueous NaHCO₃ and brine and then dried over MgSO₄. After evaporation, a yellowish crude was obtained, from which crystallized a solid (0.10 g; 0.43 mmol; 86%): [α]_D 20 –150.8° (c = 0.4, CHCl₃); The resulted compound was characterised by FITR, ¹H NMR and HRMS (FAB). All the methods confirmed the purity of the compound [18].

2.5. Preparation of immobilised complexes

Method A. The preparation of this material was done as described in [19]. Briefly, a solution of the ligand and Mn(II) chloride in methanol was added to a suspension of NaY zeolite in methanol. Triethylamine was then added and the mixture further stirred at room temperature. The solid fraction was filtered and extracted with methanol in Soxhlet apparatus. The solid sample was further washed with deionized water to remove undesired metal ions. The new material (ML-Y_A) was dried in the oven at 60 °C overnight under reduced pressure.

Method B. The preparation of this material was done as described in [19]. Briefly, NaY zeolite was first ion-exchanged with an aqueous solution of Mn(II) chloride tetrahydrate, and dried overnight under reduced pressure. Mn-Y solid was suspended in a solution of the ligand in MeOH. The mixture was stirred room temperature. The new material was filtered and washed with deionized water, ethanol and dichloromethane then dried under reduced pressure overnight. The solid was Soxhlet extracted with ethanol and after dichloromethane to remove the unreacted ligand. The new material (MnL-Y_B) was dried in the oven overnight under reduced pressure.

3. Results and discussion

Two different encapsulation procedures were used for the preparation of the heterogeneous catalysts. In both cases were expected the formation of the Mn(III) complex functionalised with 2,3-dihydropyridazine ligand. The complex formed is too large to effectively pass through the zeolite supercage free aperture (~7.4 Å), but is small enough to be confined in its large cavity (internal diameter ~12 Å) [8].

The scanning electron micrographs of NaY and the heterogeneous catalysts (not shown) indicate that there are no changes in the zeolite morphology or structure upon complex encapsulation for both catalysts [20, 21].

Chemical analyses and XRD of MnL-Y_{A/B} catalysts have confirmed the presence of metal species in the zeolite framework. Two different procedures resulted in similar manganese loading: 0.14 and 0.13 mmol g⁻¹ for catalysts obtained by methods A and B, respectively. The higher Mn/N ratio (1.71) observed for the sample obtained by method B suggests the presence of manganese ions uncoordinated to the ligand. Probably, the manganese in NaY is located

in the framework sites inaccessible to the ligand [22, 23]. Migration of some metal ions from the supercages to the sodalite cages was reported in the literature [19, 24]. The similar C/N ratio found (3.16) relates to the free complex (3.43) suggesting, that the organic ligand maintained its structure after encapsulation. Elemental analysis of the MnL-Y_A catalyst revealed the presence of a complex with a Mn/N ratio similar to the theoretical value of 1.34, calculated for the neat complex. The higher C/N obtained for MnL-Y_A (4.39) indicates the presence of the coordinated complex and of the ligand not coordinated.

The X-ray diffraction patterns of the parent zeolite (NaY) as well as Mn(III)-complex samples (MnL-Y_A and MnL-Y_B) are shown in Figs. 2 and 3, respectively. It is worth noting that X-ray phase analysis uses the peak and scan data present in the document. Reference pattern intensity and RIR values are always given for a fixed divergence slit (FDS). If the raw scan was measured with an automatic divergence slit (ADS) and the data has not been converted, then the intensity fit is not as good as possible. Therefore, for a better result the anchor scan was converted from ADS to FDS mode. One can see in Fig. 2 that no diffraction lines assigned to impurity phase were detected despite quartz which acted as an internal standard. Zeolite used as a host for manganese complexes exhibited cubic symmetry described well with a space group *Fd-3m* (No. 227) and lattice parameter: $a = 24.668(2)$ Å.

All the samples shown in Fig. 3 displayed the patterns dominated by NaY zeolite (ADS mode of presentation). However, higher weight fraction of quartz can be seen in the diffraction patterns. High intensity of diffraction lines at an angle $2\theta \approx 20.85^\circ$ and $2\theta \approx 26.63^\circ$ was due to 010/100 and 011/101 diffraction peaks of quartz exhibiting hexagonal crystal system, space group *P31 2 1* (152).

It can be assumed that the zeolite framework was not affected to a measurable extent by the exchanged manganese ions or intrazeolitic complex formation; thereby crystallinity and morphology of the zeolite NaY particles are preserved. It is clear that the X-ray diffraction patterns of the heterogeneous catalysts are not severely affected by the introduction of MnL complex in the parent zeolite structure.

All the samples were characterised also by FTIR spectroscopy (Fig. 4.). The FTIR spectrum of the NaY zeolite displays a very intense broad band at around 3450 cm^{-1} with a poorly resolved shoulder at around 3600 cm^{-1} , which can be attributed to the hydroxyl groups in supercages and in sodalite cages, respectively [25, 26] and a band at 1640 cm^{-1} , characteristic of the $\delta(\text{H}_2\text{O})$ mode of absorbed water [27]. The band at around 1020 cm^{-1} is usually attributed to the asymmetric stretching of the Al–O–Si chain of zeolite, and the symmetric stretching and bending bands of the Al–O–Si framework of zeolite appear at around 730 and 510 cm^{-1} , respectively [28]. The FTIR spectra of the heterogeneous catalysts are dominated by strong bands attributed to the parent zeolite. No shifts or broadening of the zeolite vibrational bands are observed upon encapsulation of the complex. This provides further evidence that the zeolite structure remaining unchanged after encapsulation of the complex. The intensities of bands due to the encapsulated complexes are weak because of their low loading in the zeolite structure, in agreement with the XRD analysis.

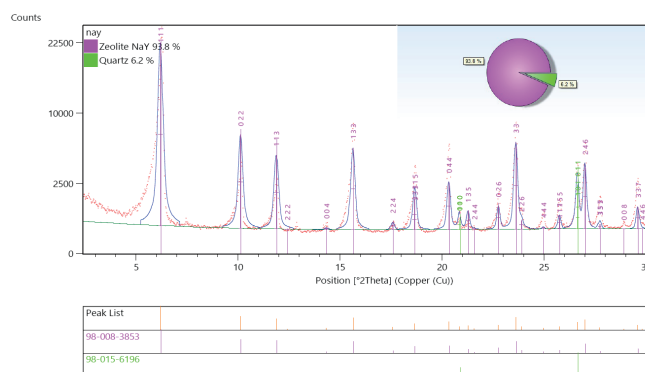


Fig. 2 XRD pattern of NaY zeolite with quartz as an internal standard. FDS mode of diffraction data presentation was chosen for better accuracy of phase analysis

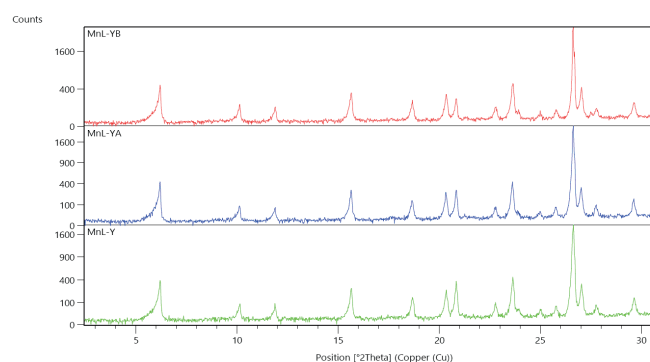


Fig. 3. XRD patterns of Mn-Y, MnL-Y_A, and MnL-Y_B. ADS mode of data presentation (i.e. as measured)

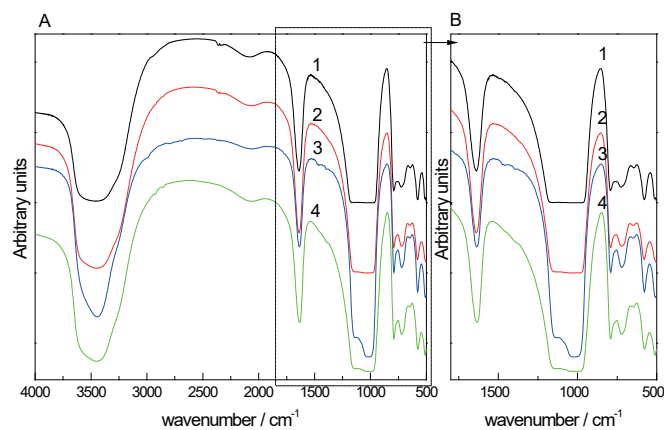


Fig. 4. FTIR spectra of 1- NaY, 2- Mn-Y, 3- MnL-YB, 4- MnL-YA in the region $4000 - 500\text{ cm}^{-1}$ (A) and $1800 - 500\text{ cm}^{-1}$ (B)

Catalytic Behaviour of the Catalysts

All heterogeneous materials were tested in catalytic oxidation of styrene because resulted epoxides are valuable building blocks in synthetic organic chemistry [12]. It is also known that styrene oxidation occurs in the presence of dioxygen with low conversion [29]. Addition of, *t*-BuOOH [13] significantly improves the oxidation efficiency as a result of a synergetic effect of both oxidants (dioxygen and *t*-BuOOH). The best oxidation conditions were obtained using DCM

Styrene oxidation in the presence of manganese complexes supported on NaY zeolite

entry	Solvent	Oxygen source	Catalyst	t (h)	%C	Epoxide		Benzaldehyde	
						S (%)	Y (%)	S (%)	Y (%)
1	ACN	tBuOOH	MnL-YB	48	49	15	8	85	41
2	ACN	tBuOOH	MnL-YA	48	40	26	10	74	30
3	DCM	tBuOOH	MnL-YB	48	60	8	5	92	55
4a)	DCM	tBuOOH	MnL-YA	48	50	4	2	90	45
5b)	Acetone	tBuOOH	MnL-YA	48	40	5	2	91	36
6	Acetone	tBuOOH	MnL-YB	48	36	0	0	100	36

Others ^{a)} S=6, Y=3; ^{b)} S=4, Y=2

as solvent. NaY and the blank experiments were performed and the same styrene conversion was observed (<1 %). A marked improvement in substrate conversion was obtained with MnL-Y_{A/B} due to the presence of the complex. Both heterogeneous catalysts lead to similar substrate conversion shown to be strongly dependent on oxygen source and less on solvent properties. The selectivity analysis shows that the benzaldehyde is a major oxidation product. The highest styrene oxide selectivity was obtained where *t*-BuOOH was used in the presence of MnL-Y_A in ACN. The catalytic results are summarised in Table 1.

In our previous paper encapsulated manganese(III) complex with salen type ligand were studied as heterogeneous catalysts for styrene epoxidation [30]. The obtained results are similar to this work. The product distribution was the same as in this work and benzaldehyde was the major oxidation product followed by styrene epoxide. No other products were detected. The conversion of styrene was similar and reaches *ca.* 40% in ACN. This behaviour suggests that the ligand properties slightly affect the catalytic properties of zeolite based catalysts. The acidity of the zeolite plays an important role in the epoxidation process. Different distribution of products was obtained when manganese complexes, salen type, immobilised on clays were used as heterogeneous catalysts. Under these conditions, the styrene oxide was the major product; nevertheless benzaldehyde was obtained in significant amount [9,31].

FTIR spectra for both heterogeneous catalysts recorded after the catalytic test does not show significant changes in measured region (not shown). It suggests that no structural changes in the zeolite matrix took place under the catalytic experimental conditions, in agreement with SEM and XRD analyses.

4. Conclusions

The manganese complex incorporating (*S*)-6-(hydroxymethyl)-*N*-phenyl-2,3-dihydropyridazine-1(6*H*)-carboxamide was encapsulated in the NaY zeolite using two different procedures: *in situ* complex preparation (A) and the flexible ligand method (B). The two procedures lead to similar manganese loading. In the catalytic studies, the heterogeneous catalysts led to similar substrate conversion which depends mainly on oxygen source but also on solvent properties. The best results were obtained using *t*-BuOOH as oxygen source and DCM as solvent.

Acknowledgement

IKB thanks to Foundation for the Science and Technology (FCT, Portugal), for the contract under 'Programa Ciência 2007 and for the contract under the project "n-SteP - Nanostructured systems for Tail" (NORTE-07-0124-FEDER-000039, supported by Norte (ON.2). FCT and FEDER (European Fund for Regional Development)-COMPETE-QREN-EU for financial support to the Research Centres, CQ/UM [PEst-C/QUI/UI0686/2013 (F-COMP-01-0124-FEDER-037302). This work is funded also by FEDER funds through the Operational Programme for Competitiveness Factors - COMPETE and by National Funds through FCT - Foundation for Science and Technology under the grant PEST-C/EQB/LA0006/2013/37285.

REFERENCES

- [1] T. Soundiressane, S. Selvakumar, S. Ménage, O. Hamelin, M. Fontecave, A.P. Singh, *J. Mol. Catal. A Chem.* 270, 132 (2007).
- [2] R. I. Kureshy, Irshad Ahmad, Noor-ul H. Khan, Sayed H.R. Abdi, Kavita Pathak, Raksh V. Jasra, *J. Catal.* 238, 134 (2006).
- [3] P. Battioni, J. P. Lallier, L. Barloy, D. Mansuny, *J. Chem. Soc., Chem. Commun.* 1149 (1989).
- [4] V. Mirkhani, M. Moghadam, S. Tangestaninejad, B. Bahramian, A. Mallekpoor-Shalamzari, *Appl. Catal., A* 321, 49 (2007).
- [5] K. Srinivasan, P. Michaud, J.K. Kochi, *J. Am. Chem. Soc.* 108, 2309 (1986).
- [6] N.H. Lee, A.R. Muci, E.N. Jacobsen, *Tetrahedron Lett.* 32, 5055 (1991).
- [7] D.E. De Vos, M. Dams, B.F. Sels, P. A. Jacobs, *Chem. Rev.* 102, 3615 (2002).
- [8] Q.-H. Fan, Y.-M. Li, A.S.C. Chan, *Chem. Rev.* 102, 3385 (2002).
- [9] I. Kuźniarska-Biernacka, A. R. Silva, A. P. Carvalho, J. Pires, C. Freire, *J. Mol. Catal. A: Chem.* 278, 82 (2007).
- [10] P. Khemthong, W. Klysubun, S. Prayoonpokarach, J. Wittayakun, *Mater. Chem. Phys.* 121, 131 (2010).
- [11] D. Feichtinger, D. A. Plattner, *Chem. Eur. J.* 7, 591 (2001).
- [12] I. Ojima, *Catalytic Asymmetric Synthesis*, VCH, New York, 1993.
- [13] A. Zsigmond, A. Horváth, F. Notheisz, *J. Mol. Catal. A: Chem.* 171, 95 (2001).
- [14] W. Adam, K. J. Roschmann, C. R. Saha-Möller, D. Seebach, *J.*

- Am. Chem. Soc. 124, 5068 (2002).
- [15] E.N. Jacobsen, M. H. Wu, in *Comprehensive Asymmetric Catalysis*, Vol. 2 (Eds.: A. Pfaltz, E. N. Jacobsen, H. Yamamoto), Springer, Berlin, 1999.
- [16] S.P. Varkey, C. Ratnasamy, P. Ratnasamy, *J. Mol. Catal. A: Chem.* 135, 295 (1998).
- [17] ICSD Database, FIZ Karlsruhe, (URL.:<http://www.fiz-karlsruhe.de>)
- [18] M.J. Alves, F.T. Costa, V.C.M. Duarte, A.G. Fortes, J.A. Martins, N.M. Micaelo, *J. Org. Chem.* 76, 9584–9592 (2011).
- [19] I. Kuźniarska-Biernacka, O. Rodrigues, M.A. Carvalho, I.C. Neves, A.M. Fonseca, *Appl. Organomet. Chem.*, 26, 44 (2012).
- [20] P. Parpot, C. Teixeira, A.M. Almeida, C. Ribeiro, I.C. Neves, A.M. Fonseca, *Micropor. Mesopor. Mater.* 117, 297 (2009).
- [21] N. Nunes, R. Amaro, F. Costa, E. Rombi, M.A. Carvalho, I.C. Neves, A.M. Fonseca, *Eur. J. Inorg. Chem.* 12, 1682 (2007).
- [22] M. Alvaro, B. Ferrer, H. Garcia, A. Sanjuan, *Tetrahedron* 55, 11895 (1999).
- [23] N. Xiao, Q. Xu, J. Sun, J. Chen, *J. Chem. Soc. Dalton Trans.* 603 (2006).
- [24] I. Kuźniarska-Biernacka, M.A. Carvalho, S.B. Rasmussen, M.A. Bañares, K. Biernacki, A. L. Magalhães, A.G. Rolo, A.M. Fonseca, I.C. Neves, *Eur. J. Inorg. Chem.* 5408 (2013).
- [25] S. Morin, P. Ayrault, N.S. Gnep, M. Guisnet, *Appl. Catal. A* 166, 281 (1998).
- [26] K. Tanaka, C.-K. Choo, Y. Komatsu, K. Hamaguchi, M. Yamaki, T. Itoh, T. Nishigaya, R. Nakata, K. Morimoto, *J. Phys. Chem. B* 108, 2501 (2004).
- [27] C. Sedlmair, B. Gil, K. Seshan, A. Jentys, J. A. Lercher, *Phys. Chem. Chem. Phys.* 5, 1897 (2003).
- [28] B. Dutta, S. Jana, R. Bera, P.K. Saha, S. Koner, *Appl. Catal. A* 318, 89 (2007).
- [29] G.V. Smith, Á. Molnár, M.M. Khan, D. Ostgard, N. Yoshida, *J. Catal.* 98, 502 (1986).
- [30] I. Kuźniarska-Biernacka, O. Rodrigues, M.A. Carvalho, P. Parpot, K. Biernacki, A.L. Magalhães, A.M. Fonseca, I. C. Neves, *Eur. J. Inorg. Chem.* 2768 (2013).
- [31] I. Kuźniarska-Biernacka, A.R. Silva, A.P. Carvalho, J. Pires, C. Freire, *Langmuir*, 21, 10825 (2005).

